Liquid Crystals
Publication details, including instructions for authors and subscription information:
http://www.informaworld.com/smpp/title~content=t713926090

The influence of flow on symmetric and asymmetric splay state relaxations

P. D. Brimicombe[a]; E. P. Raynes[a]
[a] Department of Engineering Science, University of Oxford, Oxford OX1 3PJ, UK

To cite this Article Brimicombe, P. D. and Raynes, E. P.(2005) 'The influence of flow on symmetric and asymmetric splay state relaxations', Liquid Crystals, 32: 10, 1273 — 1283
To link to this Article: DOI: 10.1080/02678290500303072
URL: http://dx.doi.org/10.1080/02678290500303072

Liquid Crystals, Vol. 32, No. 10, October 2005, 1273–1283

The influence of flow on symmetric and asymmetric splay state relaxations

P. D. BRIMICOMBE* and E. P. RAYNES
Department of Engineering Science, University of Oxford, Parks Road, Oxford OX1 3PJ, UK

(*Received 9 June 2005; accepted 20 July 2005*)

We present a detailed discussion of the relaxation of splayed states in untwisted devices — the asymmetric H state (Ha), and the recently observed symmetric H state (Hs). Experimental evidence suggests that the Hs does not experience the optical bounce due to induced backflow usually associated with splay state relaxation. A dynamic model using Leslie–Eriksen–Parodi theory has been developed, and is used to model the flow within the device during switching. We show that there is no backflow during Hs relaxation, and that the flow profile is similar to that present during relaxation of the V state (the state used for pi-cell operation). This flow enhances the switching of the Hs, leading to a faster relaxation than might be expected. The influence of the different viscosity parameters is examined in detail, and a comparison between the experimental and simulated results is given.

1. Introduction

The pi-cell [1] is generally considered to be the fastest switching nematic liquid crystal device. Originally, this device was investigated in the V state, also known as the optically compensated bend (OCB) mode. In this mode these devices have faster switching times than conventional LC displays, capable of a combined on–off response time of under 5 ms. With the advent of liquid crystal flat panel televisions, which require fast switching electro-optic devices to display high quality video information, there has been renewed interest in pi-cells [2–4]. Recently, an even faster switching mode, known as the symmetric H state, has been observed in splayed cells [5, 6]. This state has a relaxation time of around 1 ms, making it a prime candidate for high frame rate display applications.

The geometry of the splayed cell is shown in figure 1. The liquid crystal material is enclosed between two glass substrates separated by spacers. The inside surfaces of these substrates are coated with indium tin oxide (ITO), a transparent conducting material that acts as the electrodes. These surfaces are then coated with polyimide and rubbed uni-directionally. The device is assembled such that the rubbing directions are parallel, producing the surface conditions shown in figure 1 (the director is tilted by $+\theta_p$ at one surface, and $-\theta_p$ at the other).

*Corresponding author.
Email: paul.brimicombe@eng.ox.ac.uk

Figure 1 shows the commonly considered director profiles that form within pi-cell devices. With no applied voltage, the liquid crystal within the device forms a splayed ground state. Above a critical voltage V_{ca} (around $1\,V_{rms}$ for most materials), there is a Fréedericksz transition [7] into one of the asymmetric H states (Ha). As the voltage is increased further, a bend state known as the V state becomes energetically favourable (at $V_{cv} \approx 2.5\,V_{rms}$ for most materials and low pretilt devices). The H and V states are not topologically similar, so a nucleation process is required, which takes a few seconds to complete. If the voltage is allowed to fall below V_{cv} when the device is in the V state, a transient 180° twisted state forms [1], which nucleates into the H state over the course of a few seconds. Typically, the pi-cell is operated between high and low voltage V states, using it as a tunable birefringence device with the rubbing directions at 45° to crossed polarizers.

Towler and Raynes [6] observed that after short pulses of applied voltage (e.g. 2 ms burst of $6\,V_{rms}$), a splayed device exhibits a fast relaxation of around 1 ms. This fast relaxation is due to the formation of the symmetric H state (Hs), which is shown in figure 2. In simple terms, this state is similar to two half-thickness devices in the Ha (as shown in figure 2). This simplification introduces a no-slip condition at the centre of the device, which we will show is incorrect.

Most standard liquid crystal devices (i.e. Fréedericksz, TN and STN devices) are well known to experience a phenomenon known as backflow (otherwise known as the kickback effect) [1, 8–10]. When these

Liquid Crystals
ISSN 0267-8292 print/ISSN 1366-5855 online © 2005 Taylor & Francis
http://www.tandf.co.uk/journals
DOI: 10.1080/02678290500303072

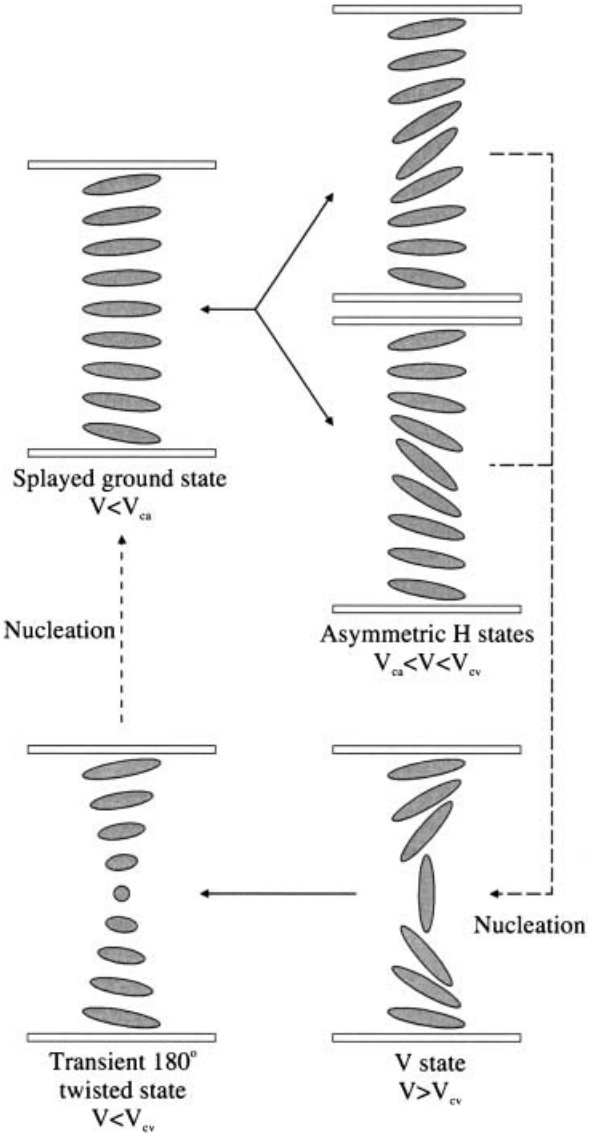

Figure 1. The commonly known states that form in splayed nematic devices. Dotted lines indicate nucleation processes.

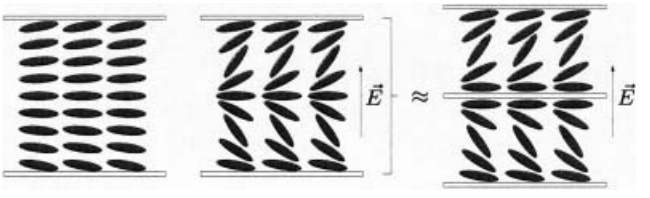

Figure 2. The symmetric H state (Hs): $V=0$ (left), $V>V_{cs}$ (centre and right). Right: simplification of the Hs as two half-thickness Fréedericksz devices.

devices relax from a high voltage state to a lower voltage state, the flow-induced torque at the centre of the device causes over-rotation of the director (i.e. it tilts past 90°) before relaxing to its final position. This produces optical bounce (a hump in the transmission curve). Bos demonstrated experimentally that the V state does not experience backflow [1], which was then confirmed by the modelling carried out by Walton and Towler [11].

2. Experimental observations

Figure 3 shows the measured transmission through a pi-cell as it relaxes from high voltage to zero voltage in both the Hs and the Ha. The device was placed with the rubbing direction at 45° to crossed polarisers, appearing bright when there is no applied voltage. The light source used was a 632.8 nm HeNe laser. Since the retardation of the device in the ground state is less than $\pi/2$, the transmission decreases monotonically as the voltage is increased. The device has a nominal thickness of 2 μm, a pretilt of 2°, and is filled with ZLI-1132 (Merck), whose material parameters are listed in table 1. The Hs relaxation was obtained by applying a 2.5 ms pulse of a 10 kHz 7 V_{rms} square wave, and the Ha by applying a 250 ms pulse of the same waveform.

Ignoring flow, the relaxation time of standard liquid crystal devices is proportional to the square of the thickness ($\tau_{rel} \propto d^2$). If the Hs behaves like two half-thickness Ha devices, then $4 \times \tau_{rel}(\text{Hs}) = \tau_{rel}(\text{Ha})$. Figure 3 (*a*) shows that the relaxation of the Hs is indeed much faster than that of the Ha. The time to the 90% level is 0.85 ms for the Hs, and 3.65 ms for the Ha. Figure 3 (*b*) shows the same data, but with the time axis of the Ha relaxation scaled by a quarter. From this plot, it is clear that the relaxation of the Ha is more than four times slower than that of the Hs (4.3 times slower to the 90% level). The non-linearity in the first millisecond of the Ha relaxation suggests that backflow is present. This non-linearity does not appear during the Hs relaxation, possibly accounting for the fact that this relaxation is more than four times faster than that of the Ha. In order to confirm this hypothesis, a dynamic model has been developed.

3. Modelling technique

The approach taken to model the device is based on Leslie–Eriksen–Parodi theory [12–14] using the van Doorn/Berreman simplification [8, 9]. Since we will only consider the H and V states in pi-cells, we can assume that there is no twist, and therefore the only variation in the director is the tilt from the horizontal, θ. The equations of motion for this system are shown below (the derivation is given in appendix A).

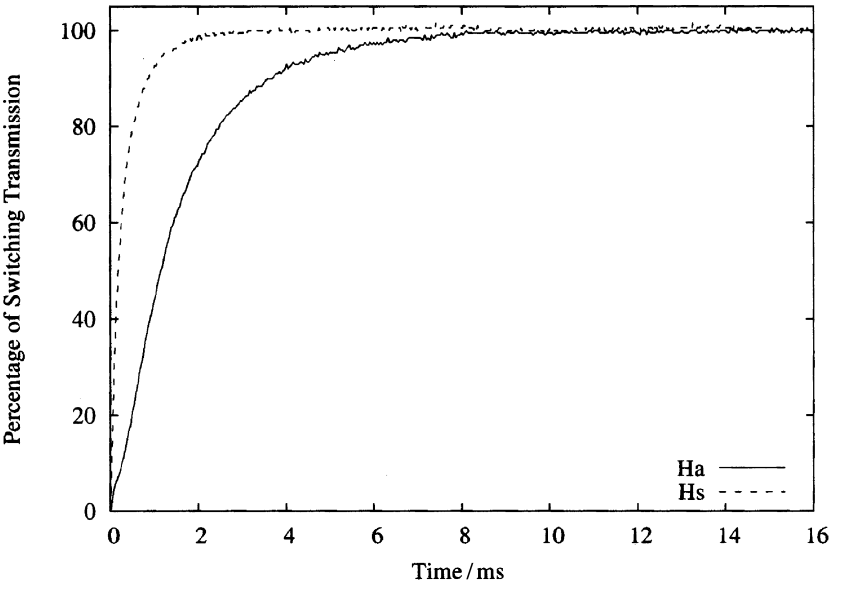

(*a*)

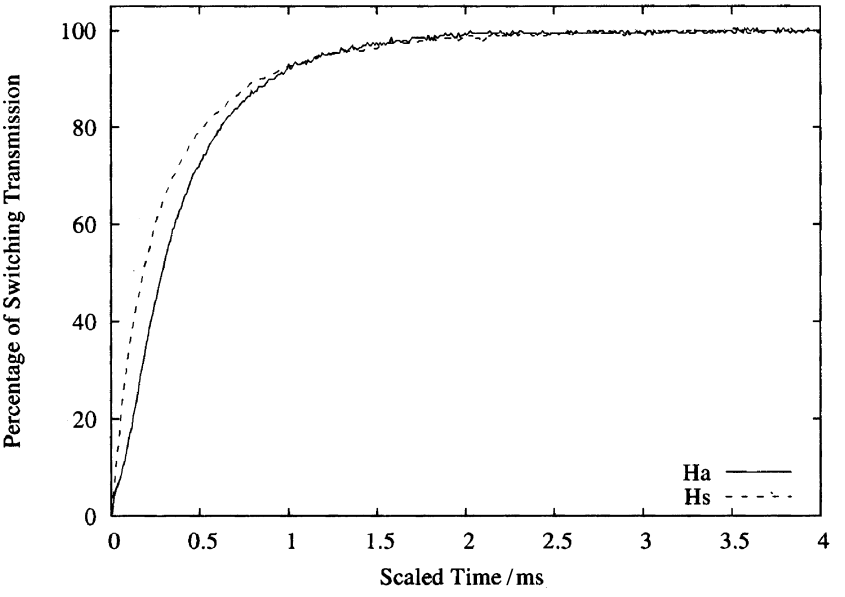

(*b*)

Figure 3. (*a*) unscaled Ha and Hs relaxations; (*b*) Ha time axis is scaled by 0.25, Hs is unscaled. Optical bounce is only present in Ha.

$$\Psi(z,\,t)=\gamma_1\dot{\theta}(z,\,t)+\beta_2(z,\,t)v_x'(z,\,t) \tag{1}$$

$$\tilde{\sigma}_{zx}(t)=\beta_2(z,\,t)\dot{\theta}(z,\,t)+\beta_1(z,\,t)v_x'(z,\,t) \tag{2}$$

where

$$\Psi(z,\,t)=\left(K_{11}\cos^2\theta+K_{33}\sin^2\theta\right)\theta''+\sin\theta\cos\theta\left[\left(K_{33}-K_{11}\right)\theta'^2+\varepsilon_0\varepsilon E_z^2(z,\,t)\right] \tag{3}$$

$$\beta_1(z,\,t)=\frac{1}{2}\left[\begin{array}{l}2\alpha_1\sin^2\theta\cos^2\theta+\alpha_2\left(\cos^2\theta-\sin^2\theta\right)\\+2\alpha_3\cos^2\theta+\alpha_4+\alpha_5\end{array}\right] \tag{4}$$

$$\beta_2(z,\,t)=\alpha_3\cos^2\theta-\alpha_2\sin^2\theta \tag{5}$$

$$\gamma_1=\alpha_3-\alpha_2. \tag{6}$$

Dashes indicate differentials with respect to z (perpendicular to the substrates), and dots indicate differentials

Table 1. The physical parameters used in the simulations [15].

Liquid crystal	Parameter	Value
ZLI-1132	K_{11}	10.8 pN
	K_{33}	26.5 pN
	$\varepsilon_{\parallel}$	17.4
	$\varepsilon_{\perp}$	4.6
	$n_{\parallel}$	1.6332
	$n_{\perp}$	1.4926
MBBA	α_1	6.5 mPa s
	α_2	−77.5 mPa s
	α_3	−1.2 mPa s
	α_4	83.2 mPa s
	α_5	46.3 mPa s

with respect to time. K_{11} and K_{33} are the liquid crystal elasticities associated with splay and bend respectively; α terms are the Leslie viscosities [12]; $\Delta\varepsilon$ is the dielectric anisotropy of the liquid crystal material; v_x is the fluid velocity in the rubbing direction; and σ_{zx} is the only non-zero component of the stress tensor (see appendix A). $E_z(z, t)$ is the local electric field in the z direction and is found from the following integral:

$$E_z(z, t) = \left(\frac{1}{\varepsilon_0 \varepsilon_{zz}}\right)\left(\frac{V}{\int_0^d \frac{\mathrm{d}z}{\varepsilon_0 \varepsilon_{zz}}}\right) \tag{7}$$

where ε_{zz} is given by

$$\varepsilon_{zz} = \varepsilon_{\perp} \cos^2\theta + \varepsilon_{\parallel} \sin^2\theta. \tag{8}$$

Assuming that the fluid velocity at the surfaces is zero, we can obtain the value of $\tilde{\sigma}_{zx}(t)$ by rearranging equation (A12) to make $v'_x(z, t)$ the subject, and integrating through the thickness of the device, d:

$$\int_0^d v'_x(z, t)\,\mathrm{d}z = 0 \tag{9}$$

$$\Rightarrow 0 = \tilde{\sigma}_{zx}(t) \int_0^d \frac{\mathrm{d}z}{\beta_1(z, t)} - \int_0^d \frac{\beta_2(z, t)\,\dot{\theta}(z, t)}{\beta_1(z, t)}\,\mathrm{d}z. \tag{10}$$

Rearranging to make $\tilde{\sigma}_{zx}(t)$ the subject,

$$\tilde{\sigma}_{zx}(t) = \frac{\int_0^d \frac{\beta_2(z, t)\dot{\theta}(z, t)}{\beta_1(z, t)}\,\mathrm{d}z}{\int_0^d \frac{\mathrm{d}z}{\beta_1(z, t)}}. \tag{11}$$

The computational process for solution is as follows.

(1) Find an initial director tilt profile, $\theta(z, 0)$ using equation (A7) with $v_{x'}$ set to zero, and guess an initial $\dot{\theta}(z, 0)$ profile (e.g. zero for all z).
(2) For the current director profile, calculate $E_z(z, t)$, $\Psi(z, t)$, $\beta_1(z, t)$, and $\beta_2(z, t)$ using equations (7), (3), (4) and (5), respectively. Find $\theta'(z, t)$ and $\theta''(z, t)$ using difference methods.
(3) Find $\tilde{\sigma}_{zx}(t)$ from equation (11).
(4) Find $v'_x(z, t)$ using equation (2).
(5) Find $\dot{\theta}(z, t)$ using equation (1).
(6) Iterate steps (3) to (5) until the value of $\tilde{\sigma}_{zx}(t)$ converges.
(7) Set $t \leftarrow t+\Delta t$; find $v_x(z, t)$ by integrating $v'_x(z, t)$; update $\theta(z, t+\Delta t)$ using an Euler method, or similar; return to step (2).

As observed by Walton and Towler [11], this process can be simplified in the case of the V state. In this state, $\beta_1(z, t)$ and $\beta_2(z, t)$ are symmetric and $\dot{\theta}(z, t)$ and $v'_x(z, t)$ are antisymmetric about the centre of the device ($z = d/2$). Thus,

$$\int_0^{\frac{d}{2}} \beta_2(z, t)\,\dot{\theta}(z, t)\,\mathrm{d}z = -\int_{\frac{d}{2}}^{d} \beta_2(z, t)\,\dot{\theta}(z, t)\,\mathrm{d}z \tag{12}$$

$$\int_0^{\frac{d}{2}} \beta_1(z, t) v'_x(z, t)\,\mathrm{d}z = -\int_{\frac{d}{2}}^{d} \beta_1(z, t) v'_x(z, t)\,\mathrm{d}z. \tag{13}$$

In this special case, integrating equation (2) with respect to z between 0 and d we have

$$\tilde{\sigma}_{zx}(t) = \frac{1}{d}\left(\int_0^d \beta_2(z, t)\dot{\theta}(z, t)\,\mathrm{d}z + \int_0^d \beta_1(z, t) v'_x(z, t)\,\mathrm{d}z\right) = 0.$$

The symmetry of the Hs also satisfies this condition. The computational process in these two cases can now be simplified by removing the iterative step to find $\tilde{\sigma}_{zx}(t)$, since its value is known, i.e. steps (3) and (6) above can be removed.

The simulations presented in this paper all use the device parameters described in § 2, and the material parameters given in table 1 unless explicitly stated. Since the viscosity parameters of ZLI-1132 have not been measured, those of MBBA have been used as a first approximation (see table 1).

4. Ha relaxation

Before the relaxation of the Ha can be modelled, the valid director profile at the high voltage state must be found. A seed profile with the correct boundary conditions

($\theta(0, t)=\theta_p$ and $\theta(d, t)=-\theta_p$) and some asymmetry about the centre of the device will converge on the Ha (if the seed profile is exactly symmetric, then the simulation will converge on the Hs, since there is nothing to drive the device into one or other of the Ha states).

Figure 4 shows a simulation of Ha relaxation from 7 V_{rms} to 0 V_{rms}. Over-rotation of the central director due to backflow [8, 9] is clearly visible from the director profile plot, figure 4 (*a*), where the director in the centre of the device rotates past the 90° tilt angle. This over-rotation causes the optical bounce in the light transmission plot, figure 4 (*c*). When the flow terms are set to zero, the optical bounce disappears, and the relaxation is smooth.

The Ha director profile is very similar to that in a Fréedericksz device (there is a slight asymmetry in the Ha profile not present in the Fréedericksz device). Unsurprisingly, therefore, the flow during Ha relaxation, figure 4 (*b*), shares many characteristics with that during Fréedericksz device relaxation [16], but with a slight asymmetry. The simulated relaxation time to the 90% level is 2.40 ms when flow is included, and 2.72 ms when it is ignored, indicating that the flow decreases the relaxation time, even though there is some backflow present.

It should be noted that backflow is only present with relaxation from relatively high applied voltages (>5 V_{rms}), when the tilt at the centre of the device approaches 90°. At lower voltages, there is no backflow, and therefore no optical bounce.

5. Hs relaxation

Figure 5 shows the Hs relaxation from 7 V_{rms} to 0 V_{rms}. The initial director profile is found using a seed profile with the same boundary conditions as the Ha, and perfect symmetry about the centre of the device. The velocity graph figure 5 (*b*), shares many features with that of the V state [11]. Since $\tilde{\sigma}_{zx}(t)=0$, as a consequence of equation (A9), and $\dot{\theta}(0, t)=\dot{\theta}(d, t)=0$ (the strong anchoring condition), $v_{x'}(0, t)=v'_x(d, t)=0$ from equation (2). This can be seen in figure 5 (*b*), since the gradient of the velocity profiles is zero at the surfaces (note that this is not the case for the Ha, since $\tilde{\sigma}_{zx}(t)$ is non-zero). Since the central director does not move in the Hs, $v_{x'}(d/2, t)$ is also zero, leading to the maximum in the flow at the centre of the device.

The presence of significant flow at $z/d=0.5$ influences the switching behaviour strongly. If the Hs behaved as two half-thickness Ha devices, then backflow would be expected in each half of the device. In fact, there is no over-rotation of the director at $z/d=0.25$ or 0.75, and the relaxation curve is smooth. The fact that the central director is free to flow prevents the backflow, and both halves of the device can relax unimpeded (regardless of the applied voltage). The simulated relaxation to the 90% switching level is 0.50 ms ms with flow, and 0.67 ms without.

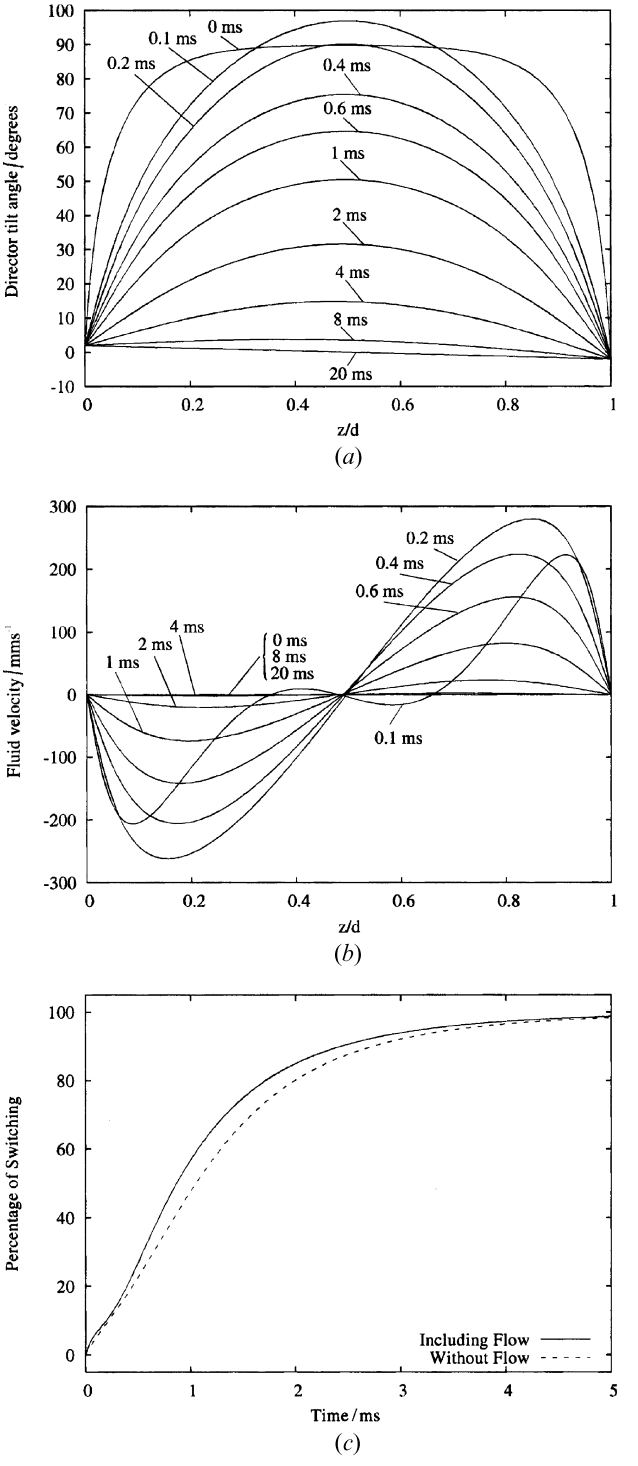

Figure 4. Ha relaxation from 7 V_{rms} to 0 V_{rms}: (*a*) director distribution, (*b*) flow profile in the device, and (*c*) switching based on light transmission.

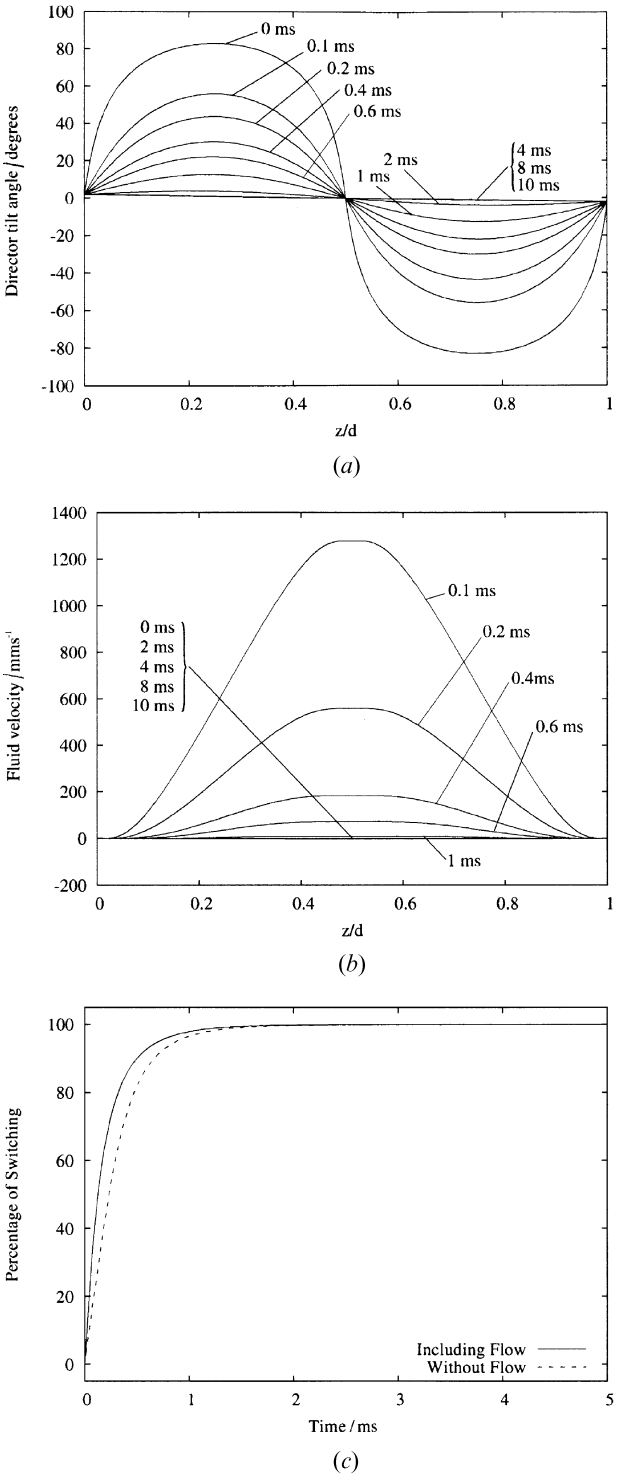

Figure 5. Hs relaxation from $7\,V_{rms}$ to $0\,_{rms}$: (*a*) director distribution, (*b*) flow profile in the device, and (*c*) switching based on light transmission.

6. Hs and Ha relaxation comparison

Figure 6 shows a comparison of the modelled transmission through the device during Hs and Ha relaxation, with the Ha time axis scaled by a quarter. Simulations where flow has been ignored are shown, as well as those where the flow has been included.

With no flow, the relaxation time of the Ha is 4.06 times slower than that of the Hs (the two transmission curves in figure 6 (*b*) are almost coincident). The reason that Ha is not four times slower, as predicted, is due to the presence of a pretilt. The Ha surface conditions are θ_p at one surface, and $-\theta_p$ at the other. If the Hs is considered as two half-thickness Ha devices, the surface conditions of each 'sub-device' are now $\pm\theta_p$ at one face, and $\theta=0$ at the other.

When flow is considered the relaxation of both states is enhanced, as could be seen in figures 4 (*c*) and 5 (*c*). This enhancement, however, is more significant in the Hs, leading to the faster than anticipated relaxation shown in figure 6 (*a*) (the relaxation time of the Ha is 4.8 times longer than that of the Hs).

7. Influence of the viscosity parameters

For ease of interpretation, the Miesowicz viscosities [17] have been used in this study as opposed to the Leslie viscosities (the relationship between the Miesowicz and Leslie viscosities is given in appendix B). There is some inconsistency in the labelling of these viscosities (particularly of η_1 and η_2), but we will use the Helfrich notation [18]. There are four shear viscosities (η_1, η_2, η_3, and the 'Helfrich coefficient' η_{12}), and one rotational viscosity (γ_1). The flows associated with these viscosities are shown in figure 7. For a calamitic nematic, $\eta_1>\eta_3>\eta_2$ because of the shape of the molecules.

Since there is no twist, η_3 does not influence the switching (during relaxation, the director has no component perpendicular to both the flow gradient and the flow direction). Typically, measured values of η_{12} are small, but can be either positive or negative (e.g. η_{12}(MBBA)=6.5 mPa s [17], η_{12}(5CB)=−6.6 mPa s [19]).Thus there are four viscosity coefficients that affect the relaxation: η_1, η_2, η_{12}, and γ_1. The influence of the vicosity parameters on the Ha and Hs relaxations are shown in figures 8 and 9. The relaxation times are highly dependent on γ_1 (the rotational viscosity), but the precise shape of the transmission curve is defined by the shear flow viscosities: η_1, η_2 and η_{12} (which has a lesser effect). The relative influence of the shear flow viscosities will be highly dependent on the applied voltage, since their effect is dependent on the director tilt angle in the device.

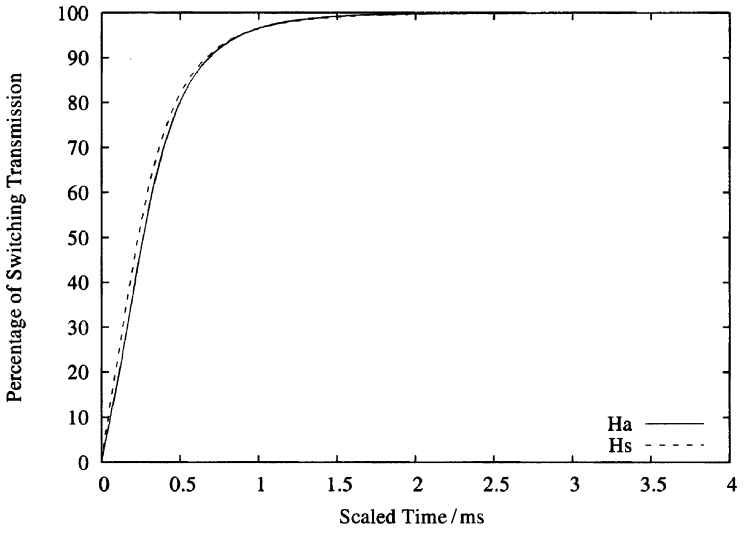

(*a*)

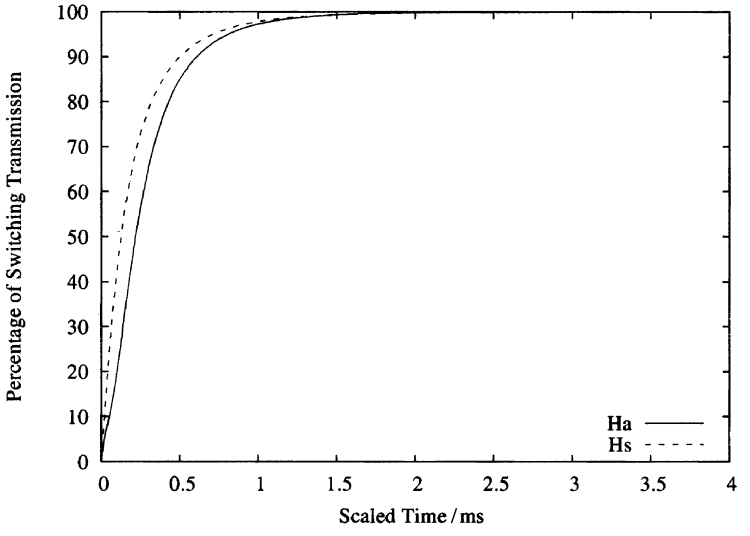

(*b*)

Figure 6. Simulated Hs and Ha relaxation comparison: (*a*) ignoring flow, and (*b*) including flow. The Ha time axes have been scaled by 0.25.

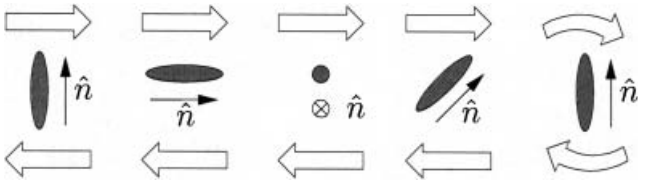

Figure 7. Flows associated with the Miesowicz viscosities. Left to right: η_1, η_2, η_3, η_4 and γ_1. The 'Helfrich coefficient' $\eta_{12}=4\eta_4-2(\eta_1+\eta_2)$. Flow is represented by the white arrows.

Figure 10 shows a comparison between the experimental relaxation curves from 7 V_{rms} shown in figure 3, and simulations using fitted viscosity coefficients. The fitted values of the viscosities found were $\eta_1=210$ mPa s, $\eta_2=10$ mPa s, $\eta_{12}=10$ mPa s, and $\gamma_1=140$ mPa s (η_3 is unknown, but will lie between η_1 and η_2). It should be noted that there is significant degeneracy between the different viscosity parameters (e.g. increasing η_1 has a similar effect to decreasing η_2), and so this is not a reliable method for measuring the viscosity parameters of the liquid crystal. In addition, there are many parameters that are not known to any significant accuracy (e.g. device thickness, pretilt angle). The fitted parameters have only been included for completeness.

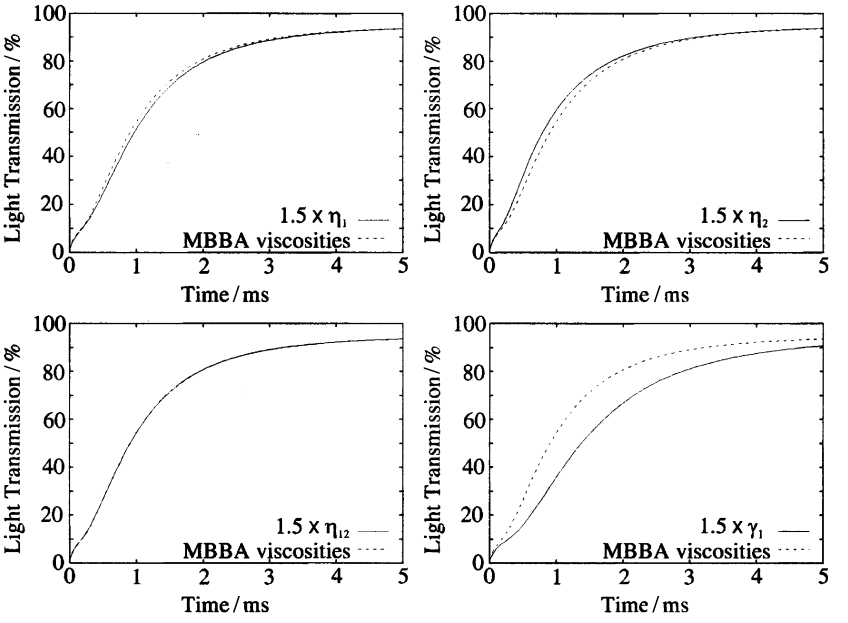

Figure 8. Simulated Hs relaxation from 7 V_{rms} to 0 V_{rms}, varying the viscosity parameters.

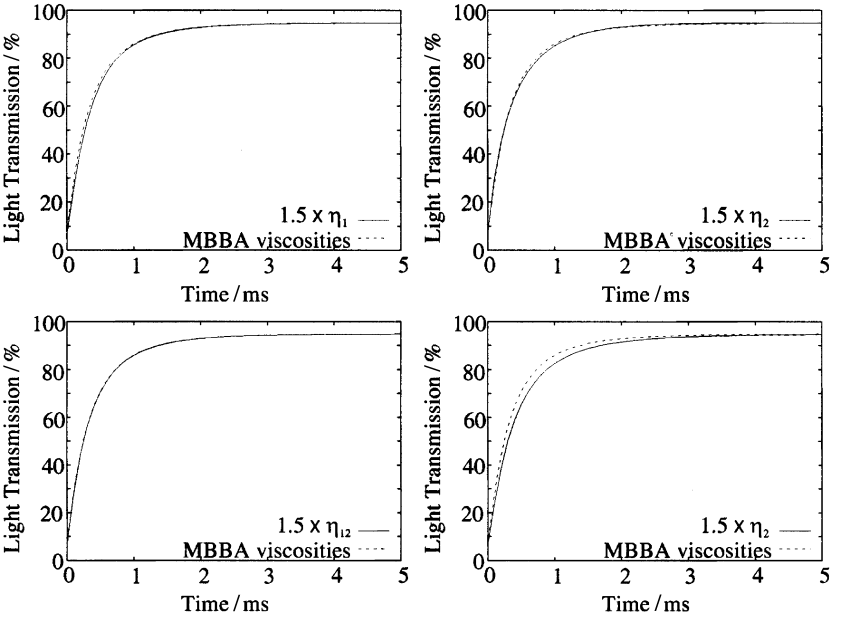

Figure 9. Simulated Ha relaxation from 7 V_{rms} to 0 V_{rms}, varying the viscosity parameters.

8. Conclusions

The relaxation of pi-cells in the H states has been shown to be highly influenced by the fluid flow during switching. We have demonstrated through experimentation and modelling that the Hs does not experience backflow during relaxation. This is due to thesymmetry of this state, which is similar to that of the V state. The Ha experiences backflow similar to that in Fréedericksz devices. The flow during Hs relaxation enhances the switching speed, leading to a faster relaxation time than would be anticipated (0.85 ms to the 90% level for a 2 μm device filled with ZLI-1132). In both the Ha and Hs, the overall relaxation time is governed by γ_1, and the precise shape of the transmission curve is influenced by both η_1 and η_2.

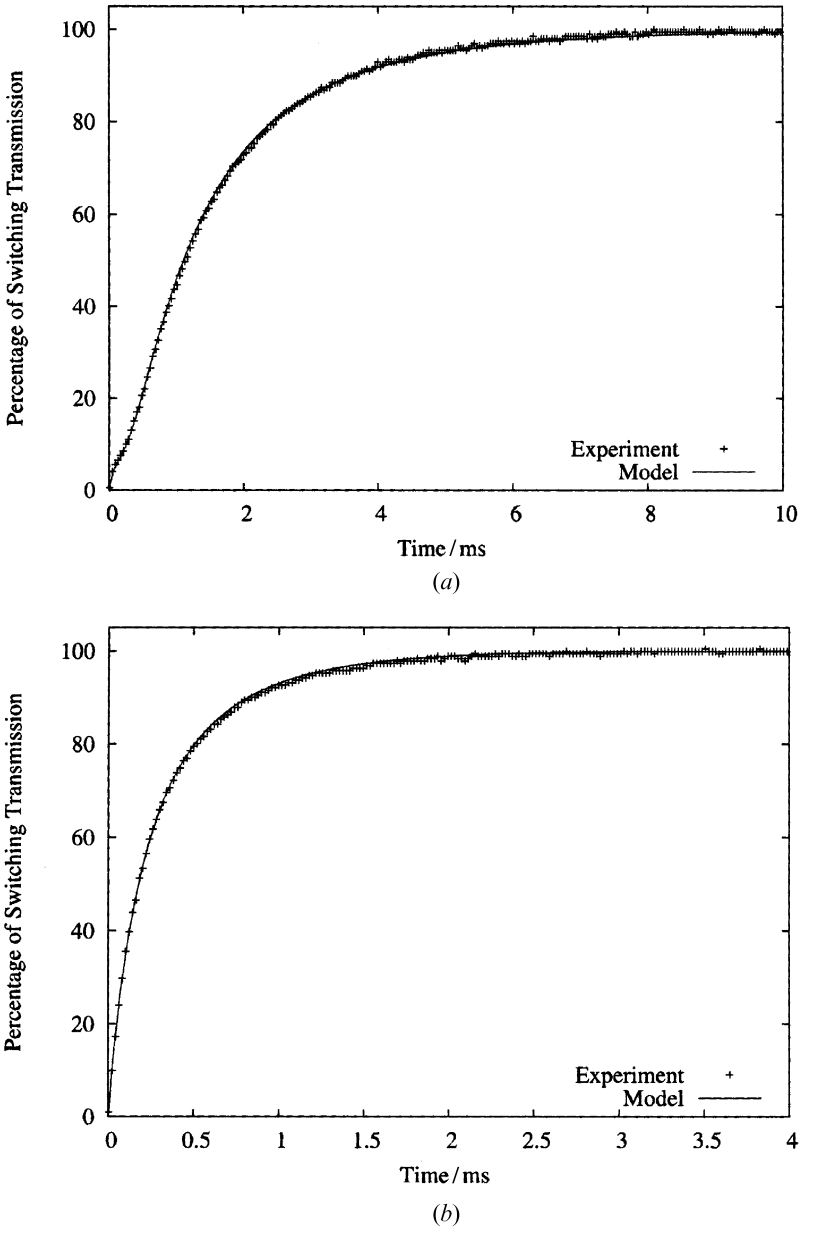

Figure 10. A comparison between experimental and simulated relaxation from $7\,V_{rms}$ to $0\,V_{rms}$: (*a*) Ha relaxation, and (*b*) Hs relaxation.

Acknowledgements

The authors would like to thank Merck UK, the COMIT Faraday Partership and the EPSRC for their financial support.

References

[1] P.J. Bos, K.R. Koehler/Beran. *Mol. Cryst. liq. Cryst.*, **113**, 329 (1984).
[2] Y. Yamaguchi, T. Miyashita, T. Uchida. *SID Dig.*, 277 (1993).
[3] T. Miyashita, Y. Yamaguchi, T. Uchida. *Jpn. J. appl. Phys.*, **34**, L177 (1995).
[4] E.J. Acosta, M.J. Towler, H.G. Walton. *Liq. Cryst.*, **27**, 977 (2000).
[5] M.J. Towler, E.P. Raynes. In *Proceedings of the 2002 International Display Research Conference* Vol 2, p.877 (2002).
[6] P.D. Brimicombe. *Investigations into a Novel Liquid Crystal Device,* final year project thesis, Oxford University (2003).
[7] V. Fréedericksz, V. Zolina. *Trans. Am. Electrochem. Soc.*, **55**, 85 (1929).
[8] C.Z. van Doorn. *J. Appl. Phys.*, **46**, 3738 (1975).

[9] D.W. Berreman. *J. Appl. Phys.*, **46**, 3746 (1975).
[10] F. Yang, Y. Dong, L.Z. Ruan, J.R. Sambles. *J. Appl. Phys.*, **96**, 310 (2004).
[11] H.G. Walton, M.J. Towler. *Liq. Cryst.*, **27**, 1329 (2000).
[12] F.M. Leslie. *Arch. Ration. Mech. Anal.*, **28**, 265 (1968).
[13] J.L. Eriksen. *Mol. Cryst. liq. Cryst.*, **7**, 153 (1969).
[14] O. Parodi. *J. Physique*, **31**, 581 (1970).
[15] P.G. de Gennes, J. Prost. *The Physics of Liquid Crystals*. Oxford University Press (1993).
[16] S. Chandraksekhar. *Liquid Crystals*. Cambridge University Press (1992).
[17] M. Miesowicz. *Nature*, **158**, 27 (1946).
[18] W. Helfrich. *J. Chem. Phys.*, **53**, 2267 (1970).
[19] G. Ahlers. In *Pattern Formation in Liquid Crystals*, Á. Buka, L. Kramer (Eds), Springer-Verlag (1995).
[20] F.C. Frank. *Discuss. Faraday Soc.*, **25**, 19 (1958).
[21] G. Vertogen, W.H. de Jeu. *Thermotropic Liquid Crystals, Fundamentals*. Springer-Verlag (1988).

Appendices

A. *Derivation of the dynamic equations*

The free energy of the system is the sum of the Frank elastic energy [20], and the electrostatic energy (ignoring flexoelectric effects and assuming strong anchoring of the director at the surfaces):

$$L=\frac{1}{2}\left[\begin{array}{l}\left(K_{11}\cos^2\theta+K_{33}\sin^2\theta\right)\left(\frac{\partial\theta}{\partial z}\right)^2\\ -E_z^2\varepsilon_0\left(\Delta\varepsilon\sin^2\theta+\varepsilon_\perp\right)\end{array}\right]. \tag{A1}$$

The calculus of variations can then be used to find the first order variation of this free energy with respect to the director tilt angle, θ. We assume that the pixel is large, so any changes in the x and y directions can be ignored:

$$\frac{\mathrm{d}L}{\mathrm{d}\theta}=\frac{\partial}{\partial z}\left(\frac{\partial L}{\partial\left(\frac{\partial\theta}{\partial z}\right)}\right)-\frac{\partial L}{\partial\theta}. \tag{A2}$$

The rate of change of the free energy of the system must equal the rate of change of dissipated energy, $\mathcal{D}$:

$$\frac{\mathrm{d}L}{\mathrm{d}t}=\frac{\mathrm{d}L}{\mathrm{d}\theta}\frac{\mathrm{d}\theta}{\mathrm{d}t}=\mathcal{D}. \tag{A3}$$

Substituting for $\mathrm{d}L/\mathrm{d}\theta$ using equation (A2) and differentiating with respect to $\mathrm{d}\theta/\mathrm{d}t$,

$$\frac{\partial}{\partial z}\left(\frac{\partial L}{\partial\left(\frac{\partial\theta}{\partial z}\right)}\right)-\frac{\partial L}{\partial\theta}=\frac{\partial\mathcal{D}}{\partial\left(\frac{\partial\theta}{\partial t}\right)}. \tag{A4}$$

The complete Rayleigh dissipation function for an anisotropic fluid is given by [21]

$$\begin{aligned}\mathcal{D}=&\frac{1}{2}\eta\left(v_{j,i}v_{j,i}+v_{j,i}v_{i,j}\right)+\frac{1}{2}\xi_1\left(n_iv_{k,i}-\dot{n}_k\right)\left(n_jv_{k,j}-\dot{n}_k\right)\\&+\frac{1}{2}\xi_2\left(n_iv_{i,k}+\dot{n}_k\right)\left(n_jv_{j,k}+\dot{n}_k\right)\\&+\xi_3\left(n_iv_{k,i}+\dot{n}_k\right)\left(n_jv_{j,k}+\dot{n}_k\right)\\&+\frac{1}{2}\xi_4n_in_jn_kn_pv_{j,i}v_{p,k},\end{aligned} \tag{A5}$$

where v_i indicates a fluid velocity in a particular direction, n_i are the components of the director, and η and ξ_i are viscosities (the usual Einstein summation convention has been used). By application of the large pixel simplification, assuming no twist, and translating the viscosity coefficients to the more widely used Leslie coefficients (see appendix B), equation (A5) simplifies to

$$\begin{aligned}\mathcal{D}=&\frac{1}{4}\left(\frac{\partial v_x}{\partial z}\right)^2\left[\begin{array}{l}2\alpha_1\sin^2\theta\cos^2\theta+\alpha_2\left(\cos^2\theta-\sin^2\theta\right)\\+2\alpha_3\cos^2\theta+\alpha_4+\alpha_5\end{array}\right]\\&+\frac{\partial v_x}{\partial z}\frac{\partial\theta}{\partial t}\left(\alpha_3\cos^2\theta-\alpha_2\sin^2\theta\right)+\frac{1}{2}\left(\frac{\partial\theta}{\partial t}\right)^2(\alpha_3-\alpha_2).\end{aligned} \tag{A6}$$

Substituting this into equation (A4), we have the full Euler–Lagrange equation including dissipative terms:

$$\begin{aligned}\dot{\theta}(\alpha_3-\alpha_2)=&\sin\theta\cos\theta\left[\left(K_{33}-K_{11}\right)\theta'^2+\varepsilon_0\Delta\varepsilon E_z^2\right]\\&+\left(K_{11}\cos^2\theta+K_{33}\sin^2\theta\right)\theta''\\&-v_x'\left(\alpha_3\cos^2\theta-\alpha_2\sin^2\theta\right)\end{aligned} \tag{A7}$$

where dashes indicate differentials with respect to z, and dots indicate differentials with respect to t. Often, flow is ignored when modelling nematic devices, and in this case, equation (A7) can be used to solve for $\dot{\theta}$ by setting $v_{x'}=0$. When flow is considered, however, there are two unknowns ($\dot{\theta}$ and $v_{x'}$), but only one equation so another equation is required.

In general, the Navier–Stokes equation for an anisotropic fluid is given by

$$\rho\dot{v}_i=F_i+\sigma_{ji,j} \tag{A8}$$

where ρ is the density of the fluid, $\dot{v}_i=\partial v_i/\partial t$, F_i is the external body force and σ_{ji} is the stress tensor. The external body forces are assumed to be negligible, so $F_i=0$. In addition, any inertial terms—the left hand side of equation (A8)—act over a timescale much shorter than the LC reorientation (the Berreman/van Doorn simplification [8, 9]). The Navier–Stokes equation, equation (A8) reduces to

$$\sigma_{ji,j}=0. \tag{A9}$$

The stress tensor can be split into two portions:

$$\sigma_{ji} = -p\delta_{ji} + \tilde{\sigma}_{ji}. \tag{A10}$$

The term $-p\delta_{ji}$ is due to the static pressure, which is assumed to be zero. $\tilde{\sigma}_{ji}$ is the dynamic portion of the stress tensor, and can be found from the Rayleigh dissipation function [21]:

$$\tilde{\sigma}_{ji} = \frac{\partial \mathcal{D}}{\partial v_{i,j}}. \tag{A11}$$

Using the Rayleigh dissipation function for the system in question, equation (A6), the only non-zero term of $\tilde{\sigma}_{ji}$ is $\tilde{\sigma}_{zx}$, and this is given by

$$\begin{aligned}\tilde{\sigma}_{zx} = \frac{1}{2} v_x' \begin{bmatrix} 2\alpha_1 \cos^2\theta \sin^2\theta + \alpha_2\left(\cos^2\theta - \sin^2\theta\right) \\ + 2\alpha_3 \cos^2\theta + \alpha_4 + \alpha_5 \end{bmatrix} \\ + \dot{\theta}\left(\alpha_3 \cos^2\theta - \alpha_2 \sin^2\theta\right).\end{aligned} \tag{A12}$$

As a consequence of equation (A9), $\tilde{\sigma}_{zx}$ must be independent of z (for each time step there is a unique value of $\tilde{\sigma}_{zx}$ which is constant for all z).

Using the following relations:

$$\begin{aligned}\Psi(z, t) = \left(K_{11}\cos^2\theta + K_{33}\sin^2\theta\right)\theta'' \\ + \sin\theta\cos\theta\left[\left(K_{33} - K_{11}\right)\theta'^2 + \varepsilon_0 \Delta\varepsilon E_z^2\right]\end{aligned} \tag{A13}$$

$$\beta_1(z, t) = \frac{1}{2}\begin{bmatrix} 2\alpha_1 \sin^2\theta\cos^2\theta + \alpha_2\left(\cos^2\theta - \sin^2\theta\right) \\ + 2\alpha_3\cos^2\theta + \alpha_4 + \alpha_5 \end{bmatrix} \tag{A14}$$

$$\beta_2(z, t) = \alpha_3\cos^2\theta - \alpha_2\sin^2\theta \tag{A15}$$

$$\gamma_1 = \alpha_3 - \alpha_2 \tag{A16}$$

we can simplify the notation of equations (A7) and (A12):

$$\Psi(z, t) = \gamma_1\dot{\theta}(z, t) + \beta_2(z, t)v_x'(z, t)$$

$$\tilde{\sigma}_{zx}(t) = \beta_2(z, t)\,\dot{\theta}(z, t) + \beta_1(z, t)v_x'(z, t). \tag{A18}$$

B. *Viscosity coefficient conversion*

The relations between the Vertogen/de Jeu viscosities and the more widely known Leslie coefficients are [21]:

$$\xi_1 = \frac{-\alpha_2 + \alpha_5}{2} \tag{A19}$$

$$\xi_2 = \frac{\alpha_2 + 2\alpha_3 + \alpha_5}{2} \tag{A20}$$

$$\xi_3 = \frac{\alpha_2 + \alpha_5}{2} \tag{A21}$$

$$\xi_4 = \alpha_1 \tag{A22}$$

$$\eta = \frac{\alpha_4}{2}. \tag{A23}$$

The relations between the Miesowicz viscosities and the Leslie coefficients are [11]:

$$\eta_1 = \frac{-\alpha_2 + \alpha_4 + \alpha_5}{2} \tag{A24}$$

$$\eta_2 = \frac{\alpha_2 + 2\alpha_3 + \alpha_4 + \alpha_5}{2} \tag{A25}$$

$$\eta_3 = \frac{\alpha_4}{2} \tag{A26}$$

$$\eta_{12} = \alpha_1 \tag{A27}$$

$$\gamma_1 = \alpha_3 - \alpha_2. \tag{A28}$$